Title
Search for $B^+ \to \ell^+ \nu_\ell$ recoiling against $B^- \to D^0 \ell^- \bar{\nu} X$

Journal
Physical Review D, 81(5)

ISSN
2470-0010

Authors
Aubert, B
Karyotakis, Y
Lees, JP
et al.

Publication Date
2010-03-01

DOI
10.1103/physrevd.81.051101

PHYSICAL REVIEW D **81,** 051101(R) (2010)

Search for $B^+ \to \ell^+ \nu_\ell$ recoiling against $B^- \to D^0 \ell^- \bar{\nu} X$

B. Aubert,[1] Y. Karyotakis,[1] J. P. Lees,[1] V. Poireau,[1] E. Prencipe,[1] X. Prudent,[1] V. Tisserand,[1] J. Garra Tico,[2] E. Grauges,[2] M. Martinelli,[3a,3b] A. Palano,[3a,3b] M. Pappagallo,[3a,3b] G. Eigen,[4] B. Stugu,[4] L. Sun,[4] M. Battaglia,[5] D. N. Brown,[5] B. Hooberman,[5] L. T. Kerth,[5] Yu. G. Kolomensky,[5] G. Lynch,[5] I. L. Osipenkov,[5] K. Tackmann,[5] T. Tanabe,[5] C. M. Hawkes,[6] N. Soni,[6] A. T. Watson,[6] H. Koch,[7] T. Schroeder,[7] D. J. Asgeirsson,[8] C. Hearty,[8] T. S. Mattison,[8] J. A. McKenna,[8] M. Barrett,[9] A. Khan,[9] A. Randle-Conde,[9] V. E. Blinov,[10] A. D. Bukin,[10,*] A. R. Buzykaev,[10] V. P. Druzhinin,[10] V. B. Golubev,[10] A. P. Onuchin,[10] S. I. Serednyakov,[10] Yu. I. Skovpen,[10] E. P. Solodov,[10] K. Yu. Todyshev,[10] M. Bondioli,[11] S. Curry,[11] I. Eschrich,[11] D. Kirkby,[11] A. J. Lankford,[11] P. Lund,[11] M. Mandelkern,[11] E. C. Martin,[11] D. P. Stoker,[11] H. Atmacan,[12] J. W. Gary,[12] F. Liu,[12] O. Long,[12] G. M. Vitug,[12] Z. Yasin,[12] V. Sharma,[13] C. Campagnari,[14] T. M. Hong,[14] D. Kovalskyi,[14] M. A. Mazur,[14] J. D. Richman,[14] T. W. Beck,[15] A. M. Eisner,[15] C. A. Heusch,[15] J. Kroseberg,[15] W. S. Lockman,[15] A. J. Martinez,[15] T. Schalk,[15] B. A. Schumm,[15] A. Seiden,[15] L. Wang,[15] L. O. Winstrom,[15] C. H. Cheng,[16] D. A. Doll,[16] B. Echenard,[16] F. Fang,[16] D. G. Hitlin,[16] I. Narsky,[16] P. Ongmongkolkul,[16] T. Piatenko,[16] F. C. Porter,[16] R. Andreassen,[17] G. Mancinelli,[17] B. T. Meadows,[17] K. Mishra,[17] M. D. Sokoloff,[17] P. C. Bloom,[18] W. T. Ford,[18] A. Gaz,[18] J. F. Hirschauer,[18] M. Nagel,[18] U. Nauenberg,[18] J. G. Smith,[18] S. R. Wagner,[18] R. Ayad,[19,†] W. H. Toki,[19] E. Feltresi,[20] A. Hauke,[20] H. Jasper,[20] T. M. Karbach,[20] J. Merkel,[20] A. Petzold,[20] B. Spaan,[20] K. Wacker,[20] M. J. Kobel,[21] R. Nogowski,[21] K. R. Schubert,[21] R. Schwierz,[21] D. Bernard,[22] E. Latour,[22] M. Verderi,[22] P. J. Clark,[23] S. Playfer,[23] J. E. Watson,[23] M. Andreotti,[24a,24b] D. Bettoni,[24a] C. Bozzi,[24a] R. Calabrese,[24a,24b] A. Cecchi,[24a,24b] G. Cibinetto,[24a,24b] E. Fioravanti,[24a,24b] P. Franchini,[24a,24b] E. Luppi,[24a,24b] M. Munerato,[24a,24b] M. Negrini,[24a,24b] A. Petrella,[24a,24b] L. Piemontese,[24a] V. Santoro,[24a,24b] R. Baldini-Ferroli,[25] A. Calcaterra,[25] R. de Sangro,[25] G. Finocchiaro,[25] S. Pacetti,[25] P. Patteri,[25] I. M. Peruzzi,[25,‡] M. Piccolo,[25] M. Rama,[25] A. Zallo,[25] R. Contri,[26a,26b] E. Guido,[26a,26b] M. Lo Vetere,[26a,26b] M. R. Monge,[26a,26b] S. Passaggio,[26a] C. Patrignani,[26a,26b] E. Robutti,[26a] S. Tosi,[26a,26b] M. Morii,[27] A. Adametz,[28] J. Marks,[28] S. Schenk,[28] U. Uwer,[28] F. U. Bernlochner,[29] H. M. Lacker,[29] T. Lueck,[29] A. Volk,[29] P. D. Dauncey,[30] M. Tibbetts,[30] P. K. Behera,[31] M. J. Charles,[31] U. Mallik,[31] J. Cochran,[32] H. B. Crawley,[32] L. Dong,[32] V. Eyges,[32] W. T. Meyer,[32] S. Prell,[32] E. I. Rosenberg,[32] A. E. Rubin,[32] Y. Y. Gao,[33] A. V. Gritsan,[33] Z. J. Guo,[33] N. Arnaud,[34] A. D'Orazio,[34] M. Davier,[34] D. Derkach,[34] J. Firmino da Costa,[34] G. Grosdidier,[34] F. Le Diberder,[34] V. Lepeltier,[34] A. M. Lutz,[34] B. Malaescu,[34] P. Roudeau,[34] M. H. Schune,[34] J. Serrano,[34] V. Sordini,[34,§] A. Stocchi,[34] G. Wormser,[34] D. J. Lange,[35] D. M. Wright,[35] I. Bingham,[36] J. P. Burke,[36] C. A. Chavez,[36] J. R. Fry,[36] E. Gabathuler,[36] R. Gamet,[36] D. E. Hutchcroft,[36] D. J. Payne,[36] C. Touramanis,[36] A. J. Bevan,[37] C. K. Clarke,[37] F. Di Lodovico,[37] R. Sacco,[37] M. Sigamani,[37] G. Cowan,[38] S. Paramesvaran,[38] A. C. Wren,[38] D. N. Brown,[39] C. L. Davis,[39] A. G. Denig,[40] M. Fritsch,[40] W. Gradl,[40] A. Hafner,[40] K. E. Alwyn,[41] D. Bailey,[41] R. J. Barlow,[41] G. Jackson,[41] G. D. Lafferty,[41] T. J. West,[41] J. I. Yi,[41] J. Anderson,[42] C. Chen,[42] A. Jawahery,[42] D. A. Roberts,[42] G. Simi,[42] J. M. Tuggle,[42] C. Dallapiccola,[43] E. Salvati,[43] R. Cowan,[44] D. Dujmic,[44] P. H. Fisher,[44] S. W. Henderson,[44] G. Sciolla,[44] M. Spitznagel,[44] R. K. Yamamoto,[44] M. Zhao,[44] P. M. Patel,[45] S. H. Robertson,[45] M. Schram,[45] P. Biassoni,[46a,46b] A. Lazzaro,[46a,46b] V. Lombardo,[46a] F. Palombo,[46a,46b] S. Stracka,[46a,46b] L. Cremaldi,[47] R. Godang,[47,‖] R. Kroeger,[47] P. Sonnek,[47] D. J. Summers,[47] H. W. Zhao,[47] X. Nguyen,[48] M. Simard,[48] P. Taras,[48] H. Nicholson,[49] G. De Nardo,[50a,50b] L. Lista,[50a] D. Monorchio,[50a,50b] G. Onorato,[50a,50b] C. Sciacca,[50a,50b] G. Raven,[51] H. L. Snoek,[51] C. P. Jessop,[52] K. J. Knoepfel,[52] J. M. LoSecco,[52] W. F. Wang,[52] L. A. Corwin,[53] K. Honscheid,[53] H. Kagan,[53] R. Kass,[53] J. P. Morris,[53] A. M. Rahimi,[53] S. J. Sekula,[53] N. L. Blount,[54] J. Brau,[54] R. Frey,[54] O. Igonkina,[54] J. A. Kolb,[54] M. Lu,[54] R. Rahmat,[54] N. B. Sinev,[54] D. Strom,[54] J. Strube,[54] E. Torrence,[54] G. Castelli,[55a,55b] N. Gagliardi,[55a,55b] M. Margoni,[55a,55b] M. Morandin,[55a] M. Posocco,[55a] M. Rotondo,[55a] F. Simonetto,[55a,55b] R. Stroili,[55a,55b] C. Voci,[55a,55b] P. del Amo Sanchez,[56] E. Ben-Haim,[56] G. R. Bonneaud,[56] H. Briand,[56] J. Chauveau,[56] O. Hamon,[56] Ph. Leruste,[56] G. Marchiori,[56] J. Ocariz,[56] A. Perez,[56] J. Prendki,[56] S. Sitt,[56] L. Gladney,[57] M. Biasini,[58a,58b] E. Manoni,[58a,58b] C. Angelini,[59a,59b] G. Batignani,[59a,59b] S. Bettarini,[59a,59b] G. Calderini,[59a,59b,¶] M. Carpinelli,[59a,59b,**] A. Cervelli,[59a,59b] F. Forti,[59a,59b] M. A. Giorgi,[59a,59b] A. Lusiani,[59a,59c] M. Morganti,[59a,59b] N. Neri,[59a,59b] E. Paoloni,[59a,59b] G. Rizzo,[59a,59b] J. J. Walsh,[59a] D. Lopes Pegna,[60] C. Lu,[60] J. Olsen,[60] A. J. S. Smith,[60] A. V. Telnov,[60] F. Anulli,[61a] E. Baracchini,[61a,61b] G. Cavoto,[61a] R. Faccini,[61a,61b] F. Ferrarotto,[61a] F. Ferroni,[61a,61b] M. Gaspero,[61a,61b] P. D. Jackson,[61a] L. Li Gioi,[61a] M. A. Mazzoni,[61a] S. Morganti,[61a] G. Piredda,[61a] F. Renga,[61a,61b] C. Voena,[61a] M. Ebert,[62] T. Hartmann,[62] H. Schröder,[62] R. Waldi,[62] T. Adye,[63] B. Franek,[63] E. O. Olaiya,[63] F. F. Wilson,[63] S. Emery,[64] L. Esteve,[64] G. Hamel de Monchenault,[64] W. Kozanecki,[64] G. Vasseur,[64] Ch. Yèche,[64] M. Zito,[64] M. T. Allen,[65] D. Aston,[65] D. J. Bard,[65] R. Bartoldus,[65] J. F. Benitez,[65] R. Cenci,[65] J. P. Coleman,[65] M. R. Convery,[65] J. C. Dingfelder,[65] J. Dorfan,[65] G. P. Dubois-Felsmann,[65] W. Dunwoodie,[65] R. C. Field,[65]

M. Franco Sevilla,[65] B. G. Fulsom,[65] A. M. Gabareen,[65] M. T. Graham,[65] P. Grenier,[65] C. Hast,[65] W. R. Innes,[65] J. Kaminski,[65] M. H. Kelsey,[65] H. Kim,[65] P. Kim,[65] M. L. Kocian,[65] D. W. G. S. Leith,[65] S. Li,[65] B. Lindquist,[65] S. Luitz,[65] V. Luth,[65] H. L. Lynch,[65] D. B. MacFarlane,[65] H. Marsiske,[65] R. Messner,[65,*] D. R. Muller,[65] H. Neal,[65] S. Nelson,[65] C. P. O'Grady,[65] I. Ofte,[65] M. Perl,[65] B. N. Ratcliff,[65] A. Roodman,[65] A. A. Salnikov,[65] R. H. Schindler,[65] J. Schwiening,[65] A. Snyder,[65] D. Su,[65] M. K. Sullivan,[65] K. Suzuki,[65] S. K. Swain,[65] J. M. Thompson,[65] J. Va'vra,[65] A. P. Wagner,[65] M. Weaver,[65] C. A. West,[65] W. J. Wisniewski,[65] M. Wittgen,[65] D. H. Wright,[65] H. W. Wulsin,[65] A. K. Yarritu,[65] C. C. Young,[65] V. Ziegler,[65] X. R. Chen,[66] H. Liu,[66] W. Park,[66] M. V. Purohit,[66] R. M. White,[66] J. R. Wilson,[66] M. Bellis,[67] P. R. Burchat,[67] A. J. Edwards,[67] T. S. Miyashita,[67] S. Ahmed,[68] M. S. Alam,[68] J. A. Ernst,[68] B. Pan,[68] M. A. Saeed,[68] S. B. Zain,[68] A. Soffer,[69] S. M. Spanier,[70] B. J. Wogsland,[70] R. Eckmann,[71] J. L. Ritchie,[71] A. M. Ruland,[71] C. J. Schilling,[71] R. F. Schwitters,[71] B. C. Wray,[71] B. W. Drummond,[72] J. M. Izen,[72] X. C. Lou,[72] F. Bianchi,[73a,73b] D. Gamba,[73a,73b] M. Pelliccioni,[73a,73b] M. Bomben,[74a,74b] L. Bosisio,[74a,74b] C. Cartaro,[74a,74b] G. Della Ricca,[74a,74b] L. Lanceri,[74a,74b] L. Vitale,[74a,74b] V. Azzolini,[75] N. Lopez-March,[75] F. Martinez-Vidal,[75] D. A. Milanes,[75] A. Oyanguren,[75] J. Albert,[76] Sw. Banerjee,[76] B. Bhuyan,[76] H. H. F. Choi,[76] K. Hamano,[76] G. J. King,[76] R. Kowalewski,[76] M. J. Lewczuk,[76] I. M. Nugent,[76] J. M. Roney,[76] R. J. Sobie,[76] T. J. Gershon,[77] P. F. Harrison,[77] J. Ilic,[77] T. E. Latham,[77] G. B. Mohanty,[77] E. M. T. Puccio,[77] H. R. Band,[78] X. Chen,[78] S. Dasu,[78] K. T. Flood,[78] Y. Pan,[78] R. Prepost,[78] C. O. Vuosalo,[78] and S. L. Wu[78]

(*BABAR* Collaboration)

[1]*Laboratoire d'Annecy-le-Vieux de Physique des Particules (LAPP), Université de Savoie, CNRS/IN2P3, F-74941 Annecy-Le-Vieux, France*
[2]*Universitat de Barcelona, Facultat de Fisica, Departament ECM, E-08028 Barcelona, Spain*
[3a]*INFN Sezione di Bari, I-70126 Bari, Italy*
[3b]*Dipartimento di Fisica, Università di Bari, I-70126 Bari, Italy*
[4]*University of Bergen, Institute of Physics, N-5007 Bergen, Norway*
[5]*Lawrence Berkeley National Laboratory and University of California, Berkeley, California 94720, USA*
[6]*University of Birmingham, Birmingham, B15 2TT, United Kingdom*
[7]*Ruhr Universität Bochum, Institut für Experimentalphysik 1, D-44780 Bochum, Germany*
[8]*University of British Columbia, Vancouver, British Columbia, Canada V6T 1Z1*
[9]*Brunel University, Uxbridge, Middlesex UB8 3PH, United Kingdom*
[10]*Budker Institute of Nuclear Physics, Novosibirsk 630090, Russia*
[11]*University of California at Irvine, Irvine, California 92697, USA*
[12]*University of California at Riverside, Riverside, California 92521, USA*
[13]*University of California at San Diego, La Jolla, California 92093, USA*
[14]*University of California at Santa Barbara, Santa Barbara, California 93106, USA*
[15]*University of California at Santa Cruz, Institute for Particle Physics, Santa Cruz, California 95064, USA*
[16]*California Institute of Technology, Pasadena, California 91125, USA*
[17]*University of Cincinnati, Cincinnati, Ohio 45221, USA*
[18]*University of Colorado, Boulder, Colorado 80309, USA*
[19]*Colorado State University, Fort Collins, Colorado 80523, USA*
[20]*Technische Universität Dortmund, Fakultät Physik, D-44221 Dortmund, Germany*
[21]*Technische Universität Dresden, Institut für Kern- und Teilchenphysik, D-01062 Dresden, Germany*
[22]*Laboratoire Leprince-Ringuet, CNRS/IN2P3, Ecole Polytechnique, F-91128 Palaiseau, France*
[23]*University of Edinburgh, Edinburgh EH9 3JZ, United Kingdom*
[24a]*INFN Sezione di Ferrara, I-44100 Ferrara, Italy*
[24b]*Dipartimento di Fisica, Università di Ferrara, I-44100 Ferrara, Italy*
[25]*INFN Laboratori Nazionali di Frascati, I-00044 Frascati, Italy*
[26a]*INFN Sezione di Genova, I-16146 Genova, Italy*
[26b]*Dipartimento di Fisica, Università di Genova, I-16146 Genova, Italy*
[27]*Harvard University, Cambridge, Massachusetts 02138, USA*
[28]*Universität Heidelberg, Physikalisches Institut, Philosophenweg 12, D-69120 Heidelberg, Germany*
[29]*Humboldt-Universität zu Berlin, Institut für Physik, Newtonstr. 15, D-12489 Berlin, Germany*
[30]*Imperial College London, London, SW7 2AZ, United Kingdom*
[31]*University of Iowa, Iowa City, Iowa 52242, USA*
[32]*Iowa State University, Ames, Iowa 50011-3160, USA*
[33]*Johns Hopkins University, Baltimore, Maryland 21218, USA*
[34]*Laboratoire de l'Accélérateur Linéaire, IN2P3/CNRS et Université Paris-Sud 11, Centre Scientifique d'Orsay, B. P. 34, F-91898 Orsay Cedex, France*

[35]*Lawrence Livermore National Laboratory, Livermore, California 94550, USA*
[36]*University of Liverpool, Liverpool L69 7ZE, United Kingdom*
[37]*Queen Mary, University of London, London, E1 4NS, United Kingdom*
[38]*University of London, Royal Holloway and Bedford New College, Egham, Surrey TW20 0EX, United Kingdom*
[39]*University of Louisville, Louisville, Kentucky 40292, USA*
[40]*Johannes Gutenberg-Universität Mainz, Institut für Kernphysik, D-55099 Mainz, Germany*
[41]*University of Manchester, Manchester M13 9PL, United Kingdom*
[42]*University of Maryland, College Park, Maryland 20742, USA*
[43]*University of Massachusetts, Amherst, Massachusetts 01003, USA*
[44]*Massachusetts Institute of Technology, Laboratory for Nuclear Science, Cambridge, Massachusetts 02139, USA*
[45]*McGill University, Montréal, Québec, Canada H3A 2T8*
[46a]*INFN Sezione di Milano, I-20133 Milano, Italy*
[46b]*Dipartimento di Fisica, Università di Milano, I-20133 Milano, Italy*
[47]*University of Mississippi, University, Mississippi 38677, USA*
[48]*Université de Montréal, Physique des Particules, Montréal, Québec, Canada H3C 3J7*
[49]*Mount Holyoke College, South Hadley, Massachusetts 01075, USA*
[50a]*INFN Sezione di Napoli, I-80126 Napoli, Italy*
[50b]*Dipartimento di Scienze Fisiche, Università di Napoli Federico II, I-80126 Napoli, Italy*
[51]*NIKHEF, National Institute for Nuclear Physics and High Energy Physics, NL-1009 DB Amsterdam, The Netherlands*
[52]*University of Notre Dame, Notre Dame, Indiana 46556, USA*
[53]*Ohio State University, Columbus, Ohio 43210, USA*
[54]*University of Oregon, Eugene, Oregon 97403, USA*
[55a]*INFN Sezione di Padova, I-35131 Padova, Italy*
[55b]*Dipartimento di Fisica, Università di Padova, I-35131 Padova, Italy*
[56]*Laboratoire de Physique Nucléaire et de Hautes Energies, IN2P3/CNRS, Université Pierre et Marie Curie-Paris 6, Université Denis Diderot-Paris7, F-75252 Paris, France*
[57]*University of Pennsylvania, Philadelphia, Pennsylvania 19104, USA*
[58a]*INFN Sezione di Perugia, I-06100 Perugia, Italy*
[58b]*Dipartimento di Fisica, Università di Perugia, I-06100 Perugia, Italy*
[59a]*INFN Sezione di Pisa, I-56127 Pisa, Italy*
[59b]*Dipartimento di Fisica, Università di Pisa, I-56127 Pisa, Italy*
[59c]*Scuola Normale Superiore di Pisa, I-56127 Pisa, Italy*
[60]*Princeton University, Princeton, New Jersey 08544, USA*
[61a]*INFN Sezione di Roma, I-00185 Roma, Italy*
[61b]*Dipartimento di Fisica, Università di Roma La Sapienza, I-00185 Roma, Italy*
[62]*Universität Rostock, D-18051 Rostock, Germany*
[63]*Rutherford Appleton Laboratory, Chilton, Didcot, Oxon, OX11 0QX, United Kingdom*
[64]*CEA, Irfu, SPP, Centre de Saclay, F-91191 Gif-sur-Yvette, France*
[65]*SLAC National Accelerator Laboratory, Stanford, California 94309 USA*
[66]*University of South Carolina, Columbia, South Carolina 29208, USA*
[67]*Stanford University, Stanford, California 94305-4060, USA*
[68]*State University of New York, Albany, New York 12222, USA*
[69]*Tel Aviv University, School of Physics and Astronomy, Tel Aviv, 69978, Israel*
[70]*University of Tennessee, Knoxville, Tennessee 37996, USA*
[71]*University of Texas at Austin, Austin, Texas 78712, USA*
[72]*University of Texas at Dallas, Richardson, Texas 75083, USA*
[73a]*INFN Sezione di Torino, I-10125 Torino, Italy*
[73b]*Dipartimento di Fisica Sperimentale, Università di Torino, I-10125 Torino, Italy*
[74a]*INFN Sezione di Trieste, I-34127 Trieste, Italy*
[74b]*Dipartimento di Fisica, Università di Trieste, I-34127 Trieste, Italy*
[75]*IFIC, Universitat de Valencia-CSIC, E-46071 Valencia, Spain*
[76]*University of Victoria, Victoria, British Columbia, Canada V8W 3P6*

[*]Deceased.
[†]Now at Temple University, Philadelphia, Pennsylvania 19122, USA.
[‡]Also with Università di Perugia, Dipartimento di Fisica, Perugia, Italy.
[§]Also with Università di Roma La Sapienza, I-00185 Roma, Italy.
[‖]Now at University of South Alabama, Mobile, Alabama 36688, USA.
[¶]Also with Laboratoire de Physique Nucléaire et de Hautes Energies, IN2P3/CNRS, Université Pierre et Marie Curie-Paris6, Université Denis Diderot-Paris7, F-75252 Paris, France.
[**]Also with Università di Sassari, Sassari, Italy.

[77]*Department of Physics, University of Warwick, Coventry CV4 7AL, United Kingdom*
[78]*University of Wisconsin, Madison, Wisconsin 53706, USA*
(Received 14 December 2009; published 30 March 2010)

We present a search for the decay $B^+ \to \ell^+ \nu_\ell (\ell = \tau, \mu, \text{ or } e)$ in $(458.9 \pm 5.1) \times 10^6$ $B\bar{B}$ pairs recorded with the *BABAR* detector at the PEP-II B-factory. We search for these B decays in a sample of B^+B^- events where one B-meson is reconstructed as $B^- \to D^0 \ell^- \bar{\nu} X$. Using the method of Feldman and Cousins, we obtain $\mathcal{B}(B^+ \to \tau^+ \nu_\tau) = (1.7 \pm 0.8 \pm 0.2) \times 10^{-4}$, which excludes zero at 2.3σ. We interpret the central value in the context of the standard model and find the B meson decay constant to be $f_B^2 = (62 \pm 31) \times 10^3$ MeV^2. We find no evidence for $B^+ \to e^+ \nu_e$ and $B^+ \to \mu^+ \nu_\mu$ and set upper limits at the 90% C.L. $\mathcal{B}(B^+ \to e^+ \nu_e) < 0.8 \times 10^{-5}$ and $\mathcal{B}(B^+ \to \mu^+ \nu_\mu) < 1.1 \times 10^{-5}$.

DOI: 10.1103/PhysRevD.81.051101 PACS numbers: 13.20.−v, 12.15.Ji, 13.25.Hw

In the standard model (SM), the purely leptonic decay $B^+ \to \ell^+ \nu_\ell$ [1] proceeds via quark annihilation into a W^+ boson. This process is related to the Cabibbo-Kobayashi-Maskawa matrix element V_{ub} and the B meson decay constant, f_B, by $\mathcal{B}(B^+ \to \ell^+ \nu_\ell) \propto |V_{ub}|^2 f_B^2$. It is also potentially sensitive to the presence of a charged Higgs boson [2], as in the minimal supersymmetric extension of the standard model. Using $|V_{ub}| = (3.94 \pm 0.26) \times 10^{-3}$ [3] and $f_B = 190 \pm 13$ MeV [4] and assuming only a SM contribution to the process, the branching fraction predictions are $\mathcal{B}(B^+ \to \tau^+ \nu_\tau) = (1.0 \pm 0.2) \times 10^{-4}$, $\mathcal{B}(B^+ \to \mu^+ \nu_\mu) = (4.5 \pm 1.0) \times 10^{-7}$, and $\mathcal{B}(B^+ \to e^+ \nu_e) = (1.1 \pm 0.2) \times 10^{-11}$. The different branching fractions result from helicity suppression of the lower-mass charged leptons. The Belle Collaboration reported evidence for the decay $B^+ \to \tau^+ \nu_\tau$ in 2006 [5]. In this paper, we describe a search for all three final states.

The data used in this analysis were collected with the *BABAR* detector at the PEP-II storage ring at the SLAC National Accelerator Laboratory. We use the full *BABAR* data set, corresponding to an integrated luminosity of 417.6 fb^{-1} with center-of-mass (CM) energy equal to the $\Upsilon(4S)$ rest mass. These data contain $(458.9 \pm 5.1) \times 10^6$ $\Upsilon(4S) \to B\bar{B}$ pairs, and we assume equal production of $B^0\bar{B}^0$ and B^+B^- from the $\Upsilon(4S)$ decays. The *BABAR* detector is described in detail elsewhere [6]. For the most recent 203 fb^{-1} of data, the barrel region of the muon system was upgraded to limited streamer tubes [7].

Signal and background processes are simulated using EVTGEN [8]. A GEANT4-based [9] Monte Carlo (MC) simulation is used to model the detector response and to estimate the signal efficiency and the physics backgrounds. Simulation samples equivalent to approximately 3 times the accumulated data were used to model $B\bar{B}$ events, and samples equivalent to approximately 1.5 times the accumulated data were used to model continuum background events where $e^+e^- \to u\bar{u}$, $d\bar{d}$, $s\bar{s}$, $c\bar{c}$, and $\tau^+\tau^-$. We independently simulate the signal processes at a rate over a hundred times that expected in data, using samples where one B meson always decays as $B^+ \to \ell^+ \nu_\ell$ and the second decays into any final state. We normalize these signal samples to their predicted SM branching fractions.

The strategy adopted for this analysis is similar to that from our previously published work [10]. Signal B decays, $B^+ \to \ell^+ \nu_\ell$, are selected in the recoil of a semileptonic decay, $B^- \to D^0 \ell^- \bar{\nu} X$, referred to as the "tag" B. The final states of the τ^+ decay in $B^+ \to \tau^+ \nu_\tau$ are identical to those in Ref. [10]: $\tau^+ \to e^+ \nu_e \bar{\nu}_\tau$, $\tau^+ \to \mu^+ \nu_\mu \bar{\nu}_\tau$, $\tau^+ \to \pi^+ \bar{\nu}_\tau$, and $\tau^+ \to \rho^+ \bar{\nu}_\tau$. For the first time, we include $B^+ \to e^+ \nu_e$ and $B^+ \to \mu^+ \nu_\mu$ in this search. In addition to using about 20% more data than in Ref. [10], we relax the constraints on the tag B, improve the definition of the discriminating variables and use a combination of tag and signal B variables in a multivariate discriminant that improves signal efficiency and background rejection.

The tag B is reconstructed in the set of semileptonic B decay modes $B^- \to D^0 \ell^- \bar{\nu} X$, through the full hadronic reconstruction of D^0 mesons and identification of the lepton, ℓ^-, as either e^- or μ^-. Other particles (X) resulting from a transition from a higher-mass charm state down to the D^0 are not explicitly reconstructed and are not included in the tag B kinematics. This strategy, and the reconstruction method (D^0 decay modes, $D^0\ell^-$ vertex requirements, etc.), are the same as in Ref. [10]. One difference in the present analysis is that we may assign up to one photon (from X) back to the tag B, based on its consistency with the decay $D^{*0} \to (\pi^0, \gamma) D^0$.

The efficiency for tag B reconstruction (ε_{tag}) is defined as the rate at which events in the signal MC are found to contain at least one reconstructed tag B and a single track recoiling against that tag. The efficiency for each signal mode is given in Table III, including corrections for systematic effects (described below). The efficiency is larger for $B^+ \to \tau^+ \nu_\tau$ events due to high-multiplicity τ^+ decays faking tag B mesons.

We identify one of the following reconstructed particles recoiling against the tag B: e^+, μ^+, π^+, or ρ^+. The e^+ and μ^+ can come from $B^+ \to \tau^+ \nu_\tau$, with the τ^+ decaying leptonically, or directly from $B^+ \to \mu^+ \nu_\mu$ or $B^+ \to e^+ \nu_e$. The signal track must originate from the interaction point (IP), with a distance of closest approach to the IP less than 2.5 cm along the beam axis and less than 1.5 cm transverse to the beam axis. We reject events that contain more than one such IP track recoiling against the tag B.

There may be additional tracks that do not come from the IP. We reject events where the single IP track is identified as a kaon. We assign the single-track recoils to categories based on a hierarchical selection. An event is assigned to the μ^+ category if the track passes muon identification or to the e^+ category if it passes electron identification; in the latter category, we recover up to one bremsstrahlung photon based on angular separation from the track and add its four-momentum to the electron's. We assign the event to the ρ^+ category if it fails lepton identification and can be paired with a π^0 candidate. The π^0 candidates used in the ρ^+ reconstruction are defined as a pair of photons, each with laboratory energy >50 MeV, with invariant mass $m_{\pi^0} = [0.115, 0.150]\ \mathrm{GeV}/c^2$. Single-track events that fail the selections above are assigned to the π^+ category.

While the direction of neither B meson can be known precisely, four-momentum conservation constrains the tag B momentum to lie on a cone around the flight direction of the reconstructed $D^0\ell^-$ system. The cosine of the opening angle between the B meson and the $D^0\ell^-$ system in the CM frame is given by

$$\cos\theta_{B,Y} = \frac{2E_B E_Y - m_B^2 - m_Y^2}{2|\vec{p}_B||\vec{p}_Y|}, \tag{1}$$

where Y refers to the reconstructed tag B final state, $(E_Y, \vec{p}_Y)$ and $(E_B, \vec{p}_B)$ are the four-momenta in the CM frame, and m_Y and m_B are the masses of the Y system and tag B^+ meson, respectively. E_B and the magnitude of $\vec{p}_B$ are calculated from the beam energy: $E_B = E_{\mathrm{CM}}/2$ and $|\vec{p}_B| = \sqrt{E_B^2 - m_B^2}$. Decays of the B meson directly to $D^0\ell^-\nu$ are largely constrained to the physical region of this cosine, while decays involving a higher-mass charm state will yield cosine values below the physical region when the intermediate decay particles (e.g. π^0 or γ) are not explicitly reconstructed.

The signal B momentum vector is equal in magnitude to $|\vec{p}_B|$ and is opposite to the tag B direction, so that it lies on the cone of the tag B momentum defined by Eq. (1). To estimate quantities in the signal B rest frame, such as the momentum of the signal B daughter(s), we choose the signal B boost vector on that cone and we compute the quantity in the corresponding rest frame. We then use the value of that quantity averaged over all trial rest frames as an estimate of the true value. We denote the momentum of the signal particle(s) determined by this method as p'_{sig}. This has the largest impact in the $B^+ \to e^+\nu_e$ and $B^+ \to \mu^+\nu_\mu$ channels, where the lepton is monoenergetic in the signal B rest frame. The improved resolution of the lepton momentum directly improves the separation of signal and background. If an event has a reconstructed signal muon (electron) candidate and $p'_{\mathrm{sig}} > 2.30(2.25)\ \mathrm{GeV}/c$, it is classified as a $B^+ \to \mu^+\nu_\mu$ ($B^+ \to e^+\nu_e$) candidate; otherwise, it is classified as $B^+ \to \tau^+\nu_\tau$, with $\tau^+ \to \mu^+\nu_\mu\bar{\nu}_\tau$ ($\tau^+ \to e^+\nu_e\bar{\nu}_\tau$).

A critical discriminating variable is the extra energy (E_{extra}), which is the total energy of charged and neutral particles that cannot be directly associated with the reconstructed daughters of the tag B or the signal B. This variable was not examined (kept "blind") until the analysis strategy was finalized. We expect the signal to concentrate near zero E_{extra}; however, due to collider-induced backgrounds, detector noise, and unassigned tracks and neutrals from the tag and signal B mesons, signal events can have nonzero E_{extra}. We require a minimum energy in the laboratory frame of 30 MeV for any neutral cluster used in E_{extra}. We improve our signal and background separation in this variable by using an algorithm to assign up to one photon from the E_{extra} back to the tag B. Candidate extra photons must have a CM-frame energy less than 300 MeV, consistent with having come from a π^0 or γ from the $D^{*0} \to D^0$ transition. If, by adding a candidate photon back to the tag B kinematics, the value of $\cos\theta_{B,Y}$ becomes closer to (but not greater than) 1.0, it is retained as a transition particle candidate. If more than one photon satisfies these conditions, the one which moves $\Delta M \equiv m_{D^0\gamma} - m_{D^0}$ closest to the nominal value of 142 MeV/c^2 [11] is used. This photon is excluded from E_{extra}. The tag B kinematic quantities and p'_{sig} are recomputed, with the photon added to the tag B final state.

The background consists primarily of B^+B^- events in which the tag B meson has been correctly reconstructed and the recoil contains one reconstructed track and additional particles that are not reconstructed. Typically these events contain K_L^0 mesons and other particles that are not detected and thus fake the multiple neutrinos in signal events. Backgrounds from B decays and continuum processes have distinctive signatures in a number of discriminating quantities. We group variables according to those which are computed from the whole event, the tag B, the signal B, and other sources. Some variables, such as those associated with the whole event, are useful for rejecting continuum background, while others (such as those associated with the reconstructed B mesons) are better at rejecting B background.

The event-level variables are: the ratio of the second and zeroth Fox-Wolfram moments [12]; the minimum invariant mass of any two charged tracks in the event; the net charge of the event; $\cos\theta_{B,Y}$; the invariant mass of the two leptons in the event ($m_{\ell\ell}$); and the missing mass vs cosine of the polar angle (laboratory frame) of the missing three-momentum, where the sum defining the reconstructed four-momentum runs over all charged and neutral particles in the event. The tag B variables are: the D^0 decay mode; the CM momenta of the tag B kaon and lepton; particle identification quality of the tag B charged kaon (where applicable). The signal B variables are: the quality of the particle identification of the signal muon, for muon final states of the signal B; the quality of the kaon identification on the signal track (to reject kaons misidentified as leptons

or pions); for $\tau^+ \to \pi^+\pi^0\bar{\nu}_\tau$, the reconstructed mass of the ρ^+, and the CM momenta of the ρ^+ daughters; and for $B^+ \to \tau^+\nu_\tau$, $\cos\theta'_{\tau,Y}$ vs $p'_{\rm sig}$, where $\cos\theta'_{\tau,Y}$ is defined in the signal B meson rest frame using Eq. (1), replacing B meson quantities with those of the τ ($E_\tau = m_B/2$ and $p_\tau = \sqrt{m_B^2 - m_\tau^2}$) and where Y refers to the reconstructed τ final state (computed using the signal B meson rest frame averaging procedure). Other variables used are: the separation between the tag B meson decay vertex and the point of closest approach to the IP by the signal B track; and the distribution of the cosine of the angle between the signal B CM momentum and the tag B thrust vs the minimum invariant mass of any three charged particles in the event [10].

The shapes of these variables in MC simulation are then used to define probability density functions (PDFs) for signal (P_s) and background (P_b). We define for each variable the ratio $P_s/[P_b + P_s]$. We use the product of these ratios to construct a pair of likelihood ratios (LHRs) for each signal channel, one for rejecting B backgrounds ($\mathrm{LHR}_{B\bar{B}}$) and the other for rejecting continuum ($\mathrm{LHR}_{\rm cont}$) backgrounds. The LHR output is bounded between 0 and 1, with signal accumulating toward 1 and background toward 0.

We optimize selection criteria on $E_{\rm extra}$, $\mathrm{LHR}_{B\bar{B}}$, and $\mathrm{LHR}_{\rm cont}$ for all modes. For the $B^+ \to e^+\nu_e$ and $B^+ \to \mu^+\nu_\mu$ modes, we additionally optimize the selection on $p'_{\rm sig}$. For the $\tau^+ \to e^+\nu_e\bar{\nu}_\tau$ mode we additionally optimize the selection on $m_{\ell\ell}$ (to reject poorly modeled photon-conversion background). For the τ decay modes, we choose the figure-of-merit (FOM) to be $N_{\rm sig}/\sqrt{(N_{\rm sig} + N_{\rm bg})}$, since there is still significant background left in these channels even after final selection criteria are applied. For $B^+ \to \mu^+\nu_\mu$ and $B^+ \to e^+\nu_e$ we use $N_{\rm sig}/(3/2 + \sqrt{N_{\rm bg}})$ [13] due to the low expected background. We divide the MC simulation samples for signal and background into thirds, two for optimization and one from which to compute unbiased efficiencies and background predictions. This latter sample has statistics roughly equivalent to the data. Optimized selection criteria are given in Table I. The signal efficiency ($\varepsilon_{\rm sig}$) is defined as the rate at which signal events containing a reconstructed tag B are also found to contain a signal B candidate, and it includes the τ^+ branching fractions. These efficiencies are given in Table III.

We calibrate our background prediction using sideband regions of $E_{\rm extra}$ where the signal contribution is negligible. We define the sidebands for $B^+ \to \tau^+\nu_\tau$, $B^+ \to \mu^+\nu_\mu$, and $B^+ \to e^+\nu_e$ as $E_{\rm extra} \geq 0.4$ GeV, ≥ 0.72 GeV, and ≥ 0.6 GeV, respectively. We predict $\mathcal{N}_{\rm bg}^{\rm data}$, the number of background events in data in the $E_{\rm extra}$ signal region (Table II), by scaling the yield predicted by the MC simulation ($N_{\rm bg}^{\rm MC}$) by the ratio of yields in data ($N_{\rm side}^{\rm data}$) and MC ($N_{\rm side}^{\rm MC}$) in the sideband. This method assumes that the shape of $E_{\rm extra}$ is well described but does not rely on the absolute prediction of the yield. We validate this approach by defining sidebands in other variables (D^0 mass, $\mathrm{LHR}_{\rm cont}$, $\mathrm{LHR}_{B\bar{B}}$, and $p'_{\rm sig}$) and studying the data/MC agreement for the entire $E_{\rm extra}$ background shape. We find the shape to be well described. We also studied the effect of varying the $E_{\rm extra}$ sideband definition and obtained consistent background predictions.

TABLE I. Optimized signal selection criteria.

Mode	$\mathrm{LHR}_{B\bar{B}}$	$\mathrm{LHR}_{\rm cont}$	$E_{\rm extra}$ (GeV)	$p'_{\rm sig}$ (GeV/c)	$m_{\ell\ell}$ (GeV/c^2)
$B^+ \to \tau^+\nu_\tau$					
$e^+\bar{\nu}\nu$	>0.77	>0.25	<0.20	···	>0.29
$\mu^+\bar{\nu}\nu$	>0.14	>0.72	<0.24	···	···
$\rho^+\nu$	>0.97	>0.95	<0.24	···	···
$\pi^+\nu$	>0.57	>0.80	<0.35	···	···
$B^+ \to (\mu^+, e^+)\nu$					
$\mu^+\nu$	>0.33	>0.61	<0.72	[2.45, 2.98]	···
$e^+\nu$	None	>0.01	<0.57	[2.52, 3.02]	···

TABLE II. Background predictions from the $E_{\rm extra}$ sideband, as described in the text.

Mode	$N_{\rm side}^{\rm MC}$	$N_{\rm side}^{\rm data}$	$N_{\rm bg}^{\rm MC}$	$\mathcal{N}_{\rm bg}^{\rm data}$
$\tau^+ \to e^+\nu_e\bar{\nu}_\tau$	333 ± 19	334 ± 18	81 ± 10	81 ± 12
$\tau^+ \to \mu^+\nu_\mu\bar{\nu}_\tau$	1248 ± 36	1236 ± 35	136 ± 12	135 ± 13
$\tau^+ \to \pi^+\bar{\nu}_\tau$	6507 ± 88	7167 ± 85	212 ± 19	234 ± 19
$\tau^+ \to \rho^+\bar{\nu}_\tau$	1841 ± 48	1734 ± 42	62 ± 9	59 ± 9
$B^+ \to \mu^+\nu_\mu$	12 ± 5	14 ± 4	12 ± 5	13 ± 8
$B^+ \to e^+\nu_e$	26 ± 6	42 ± 6	15 ± 5	24 ± 11

TABLE III. The corrected tag and signal efficiencies. The first uncertainty is the MC statistical uncertainty, and the second is the systematic uncertainty from sources described in the text. Branching fractions are included (e.g. $\tau^+ \to e^+ \nu \bar{\nu}$). The last column is the total systematic uncertainty on each efficiency as a percent of its value.

Channel	Efficiency (%)	Uncertainty (%)
Tag efficiencies		
$B^+ \to \tau^+ \nu_\tau$	$(1.514 \pm 0.003 \pm 0.107)$	7.1
$B^+ \to \mu^+ \nu_\mu$	$(0.937 \pm 0.003 \pm 0.066)$	7.1
$B^+ \to e^+ \nu_e$	$(0.974 \pm 0.003 \pm 0.069)$	7.1
Signal efficiencies		
$\tau^+ \to e^+ \nu_e \bar{\nu}_\tau$	$(1.58 \pm 0.04 \pm 0.07)$	4.5
$\tau^+ \to \mu^+ \nu_\mu \bar{\nu}_\tau$	$(1.45 \pm 0.03 \pm 0.11)$	7.4
$\tau^+ \to \pi^+ \bar{\nu}_\tau$	$(2.44 \pm 0.05 \pm 0.11)$	4.5
$\tau^+ \to \rho^+ \bar{\nu}_\tau$	$(0.83 \pm 0.03 \pm 0.05)$	5.4
$B^+ \to \tau^+ \nu_\tau$	$(6.31 \pm 0.07 \pm 0.34)$	5.4
$B^+ \to \mu^+ \nu_\mu$	$(28.65 \pm 0.34 \pm 1.75)$	6.1
$B^+ \to e^+ \nu_e$	$(37.01 \pm 0.38 \pm 1.84)$	5.0

The branching fraction for any of the decay modes is

$$\mathcal{B}(B^+ \to \ell^+ \nu_\ell) = \frac{N_{\rm obs} - \mathcal{N}_{\rm bg}^{\rm data}}{2 N_{B^+B^-} \varepsilon_{\rm tag} \varepsilon_{\rm sig}}, \tag{2}$$

where $N_{\rm obs}$ is the total number of events observed in the signal region and $N_{B^+B^-}$ is the total number of $\Upsilon(4S) \to B^+B^-$ decays in the data. The estimation of $N_{B^+B^-}$ has an uncertainty of 1.1% [14].

Potential sources of significant systematic uncertainty in $\varepsilon_{\rm tag}$ and $\varepsilon_{\rm sig}$ include the tag reconstruction rate, the modeling of $E_{\rm extra}$, and signal track and neutral reconstruction. We use "double-tagged" events to study possible effects. Double-tagged events contain two fully reconstructed, independent, oppositely charged semileptonic tag B decays. These double-tagged events are analogous to signal, in that every particle that can be assigned to the original B decays has been assigned.

We use the absolute yields of tagged events to obtain a systematic uncertainty on $\varepsilon_{\rm tag}$. We form a double ratio from the ratios of double-tagged to single-tagged events in the data and MC simulation. Single-tagged events are defined as events containing at least one semileptonic tag B decay with no constraints on the rest of the event. We improve the sample purity by requiring that $D^0 \to K^- \pi^+$ in at least one of the tags. We measure this double ratio to be 0.891 ± 0.021. As a comparison, we perform the same measurement replacing $D^0 \to K^- \pi^+$ with $D^0 \to K^- \pi^+ \pi^- \pi^+$ and find the double-ratio to be 0.954 ± 0.011. We use 0.891 as the nominal correction to $\varepsilon_{\rm tag}$ and treat the relative difference between the two methods (7.1%) as the systematic uncertainty.

The $E_{\rm extra}$ distribution in double-tag events is expected to contain contributions similar, though not identical, to those from signal events. We validate $E_{\rm extra}$ using the double-tagged events described above, additionally requiring that the second tag contains only $D^0 \to K^- \pi^+$ and satisfies $\cos\theta_{B,Y} = [-1.1, 1.1]$ to reject second tags with missing neutrals. The resulting $E_{\rm extra}$ distribution is shown in Fig. 1. It is well-described by the MC simulation. We compare the efficiency of selecting events in data and MC simulation for $E_{\rm extra} \leq 0.4$ GeV and find that the efficiency needs to be corrected by 0.985 ± 0.044 to match the data. The uncertainty on this correction is due to the statistical uncertainty on the data and MC simulation, and we treat it as a systematic uncertainty.

The remaining systematic uncertainties on $\varepsilon_{\rm sig}$ come from tracking efficiency (0.36% per signal track), π^0 reconstruction for the $\tau^+ \to \rho^+ \bar{\nu}_\tau$ mode (0.984 ± 0.030), and particle identification. These are evaluated using control samples of well-characterized particles. The particle identification efficiency corrections and systematic uncertainties are 0.953 ± 0.003 (0.97 ± 0.04) for identified electrons in the $B^+ \to \tau^+ \nu_\tau$ ($B^+ \to e^+ \nu_e$) analysis and 0.92 ± 0.05 (1.016 ± 0.022) for identified muons in the $B^+ \to \tau^+ \nu_\tau$ ($B^+ \to \mu^+ \nu_\mu$) analysis.

The $E_{\rm extra}$ distributions for each channel are given in Fig. 2 and results given in Table IV. We use the method of Feldman and Cousins [15] to interpret the yields in each channel. When computing the level at which we exclude the null hypothesis, we include systematic errors as a Gaussian convolution with the nominal Poisson distribution. Our results in the $B^+ \to \mu^+ \nu_\mu$ and $B^+ \to e^+ \nu_e$ channels are consistent with the background expectation and we obtain only one-sided 90% confidence intervals. For $B^+ \to \tau^+ \nu_\tau$, we obtain a two-sided 68% confidence interval and exclude the null hypothesis at the level of 2.3σ. This result supersedes that of the previous work [10]. The statistical consistency test of the results over the four $B^+ \to \tau^+ \nu_\tau$ channels has a χ^2 per degree-of-

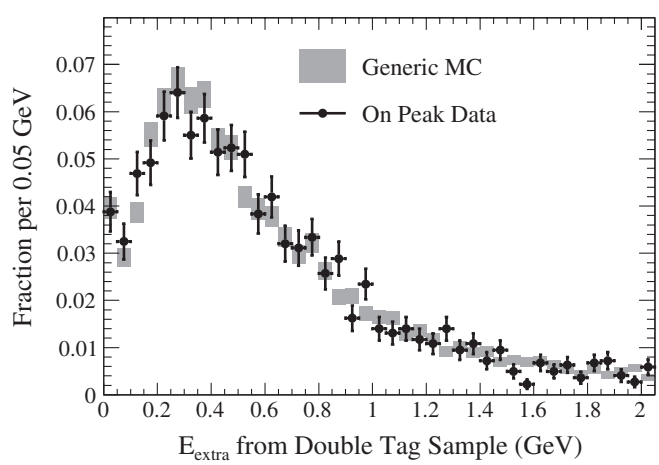

FIG. 1. Distribution of $E_{\rm extra}$ in double-tagged events. The data (black points) and MC simulated events (gray rectangles) are normalized to unit area. The rectangles represent the MC simulation uncertainty.

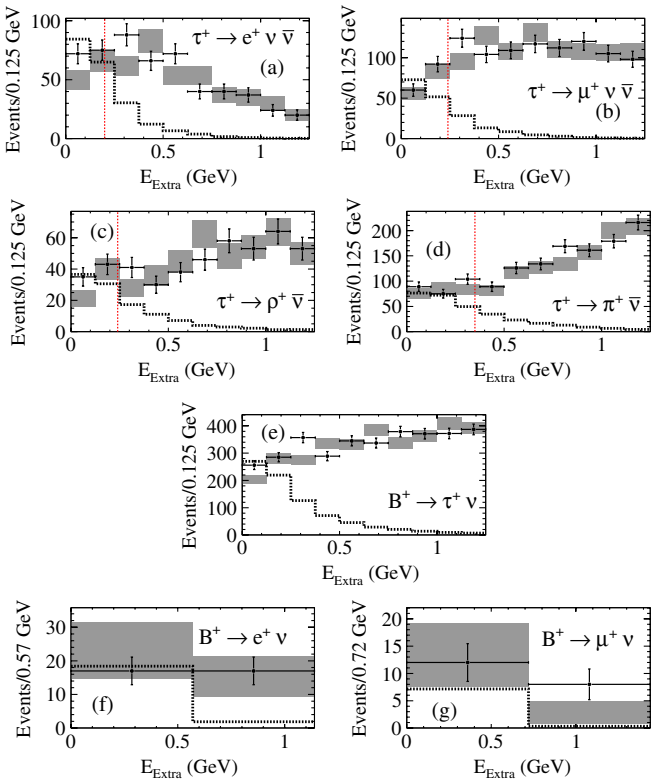

FIG. 2 (color online). $E_{\rm extra}$ after all selection criteria have been applied for each final state. Shown are data (black points), background MC simulation (gray shaded), and signal MC simulation (dotted line) normalized to 10 times the expected branching fraction (10^6 times for $B^+ \to e^+ \nu_e$). The background MC simulation is luminosity normalized and corrected for the data/MC ratio in the $E_{\rm extra}$ sideband; the rectangles represent the MC simulation statistical uncertainty. In (a–d), the vertical dashed line indicates the signal region boundary. In (f–g) the first bin is the signal region.

freedom of 2.02/3, or a probability of 57%, and is performed using branching fractions computed with Eq. (2). In the context of the SM, we determine that $f_B^2 = (62 \pm 31) \times 10^3$ MeV^2, where the uncertainty arises dominantly from this measurement and $|V_{ub}|$.

We obtain a single *BABAR* result for $B^+ \to \tau^+ \nu_\tau$ by combining this result with $\mathcal{B}(B^+ \to \tau^+ \nu_\tau) = (1.8^{+1.0}_{-0.9}) \times 10^{-4}$, which is derived from a statistically-independent sample using tag B mesons decaying into fully hadronic final states [16]. We use a simple error-weighted average, since the correlated systematics (mainly due to particle identification, charged particle tracking, and $E_{\rm extra}$) have a negligible impact on the combination. We obtain $\mathcal{B}(B^+ \to \tau^+ \nu_\tau) = (1.7 \pm 0.6) \times 10^{-4}$, which excludes zero at the 2.8σ level. Both this and the combined results are consistent with the SM prediction.

TABLE IV. The expected background, observed events in data, and branching fraction results, determined as described in the text.

Mode	$\mathcal{N}_{\rm bg}^{\rm data}$	$N_{\rm obs}$	Branching fraction ($\times 10^{-4}$)
$\tau^+ \to e^+ \nu_e \bar{\nu}_\tau$	81 ± 12	121	(3.6 ± 1.4)
$\tau^+ \to \mu^+ \nu_\mu \bar{\nu}_\tau$	135 ± 13	148	$(1.3^{+1.8}_{-1.6})$
$\tau^+ \to \rho^+ \bar{\nu}_\tau$	59 ± 9	71	$(2.1^{+2.0}_{-1.8})$
$\tau^+ \to \pi^+ \bar{\nu}_\tau$	234 ± 19	243	$(0.6^{+1.4}_{-1.2})$
$B^+ \to \tau^+ \nu_\tau$	509 ± 30	583	$(1.7 \pm 0.8 \pm 0.2)$
$B^+ \to \mu^+ \nu_\mu$	13 ± 8	12	<0.11 (90% C.L.)
$B^+ \to e^+ \nu_e$	24 ± 11	17	<0.08 (90% C.L.)

In conclusion, we have used the complete *BABAR* data sample to search for the purely leptonic B meson decay $B^+ \to \ell^+ \nu$ using a semileptonic B decay tagging technique. We measure $\mathcal{B}(B^+ \to \tau^+ \nu_\tau) = (1.7 \pm 0.8 \pm 0.2) \times 10^{-4}$ and exclude the null hypothesis at the level of 2.3σ. We find results consistent with the background predictions for the decays $B^+ \to \mu^+ \nu_\mu$ and $B^+ \to e^+ \nu_e$. We are grateful for the excellent luminosity and machine conditions provided by our PEP-II colleagues, and for the substantial dedicated effort from the computing organizations that support *BABAR*. The collaborating institutions wish to thank SLAC for its support and kind hospitality.

This work is supported by DOE and NSF (USA), NSERC (Canada), CEA and CNRS-IN2P3 (France), BMBF and DFG (Germany), INFN (Italy), FOM (The Netherlands), NFR (Norway), MES (Russia), MEC (Spain), and STFC (United Kingdom). Individuals have received support from the Marie Curie EIF (European Union) and the A. P. Sloan Foundation.

[1] Charge-conjugate modes are implied throughout this paper.
[2] W.-S. Hou, Phys. Rev. D **48**, 2342 (1993).
[3] E. Barberio *et al.* (Heavy Flavor Averaging Group), arXiv:0808.1297.
[4] E. Gamiz, C. T. H. Davies, G. P. Lepage, J. Shigemitsu, and M. Wingate (HPQCD Collaboration), Phys. Rev. D **80**, 014503 (2009).
[5] K. Ikado *et al.* (Belle Collaboration), Phys. Rev. Lett. **97**, 251802 (2006).
[6] B. Aubert *et al.* (*BABAR* Collaboration), Nucl. Instrum. Methods Phys. Res., Sect. A **479**, 1 (2002).
[7] W. Menges, IEEE Nucl. Sci. Symp. Rec. **5**, 1470 (2006).
[8] D. J. Lange, Nucl. Instrum. Methods Phys. Res., Sect. A **462**, 152 (2001).
[9] S. Agostinelli *et al.* (GEANT4 Collaboration), Nucl. Instrum. Methods Phys. Res., Sect. A **506**, 250 (2003).
[10] B. Aubert *et al.* (*BABAR* Collaboration), Phys. Rev. D **76**,

052002 (2007).

[11] C. Amsler *et al.* (Particle Data Group), Phys. Lett. B **667**, 1 (2008).

[12] G. C. Fox and S. Wolfram, Phys. Rev. Lett. **41**, 1581 (1978).

[13] G. Punzi, *Proceedings of PHYSTAT2003: Statistical Problems in Particle Physics, Astrophysics, and Cosmology* (2003), pp. 79–83.

[14] B. Aubert *et al.* (*BABAR* Collaboration), Phys. Rev. D **67**, 032002 (2003).

[15] G. J. Feldman and R. D. Cousins, Phys. Rev. D **57**, 3873 (1998).

[16] B. Aubert *et al.* (*BABAR* Collaboration), Phys. Rev. D **77**, 011107 (2008).